

**Nitrate Photolysis in Snow**

Theodore Tran

Dr. Ted Hullar

Dr. Cort Anastasio

UC Davis Department of Land, Air, & Water Resources

**Abstract**

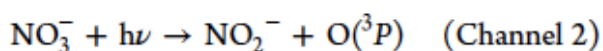
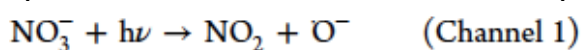
*Snow is an important medium in photochemistry as light can penetrate several tens of centimeters and release reaction products into the atmosphere. One chemical is nitrate ( $\text{NO}_3^-$ ) which undergoes photolysis to form nitrite ( $\text{NO}_2^-$ ) and atmospheric oxidants thus influences their concentration. However, current data on nitrate reactivity is unclear since it can be found in three areas: within the solid ice matrix, the liquid-like region (grain boundaries of the ice matrix), and at the air-ice interface. Past efforts show that photolysis of nitrate occurs faster at the air-ice interface compared to the liquid-like region and aqueous solution but studies have not observed this reaction in a relevant environment that is approximate to snow. Simply freezing water is not nature identical to real life conditions therefore we have built a snow-making machine to: incorporate principles of supersaturate water vapors, form snow crystals, and ultimately vapor deposit  $\text{NO}_3^-$ . The snow is then exposed to simulated polar sunlight via a filtered arc lamp and is tested for nitrate's decay rate. We hope to find the rate at which  $\text{NO}_3^-$  is photolyzed into atmospheric oxidants in real life conditions however we had issues with  $\text{NO}_2^-$  contamination during snow production and our light source did not induce any photochemistry. Fortunately, we were able to reduce  $\text{NO}_2^-$  contamination by running the snow machine for 96 hours a week and have started to use a new light source, MIS monochromator. Preliminary result for  $\text{NO}_2^-$  quantum yield is 1.82% +/- 0.78 but more experiments are needed to confirm this result.*

# 1. Introduction

The photolysis of nitrate ( $\text{NO}_3^-$ ) in snow produces nitrogen oxides ( $\text{NO}_x$ ) and nitrous acid ( $\text{HONO}$ ),<sup>14</sup> which can form near-surface ozone and hydroxyl radicals, respectively.<sup>1,4,5,8,13,19,25</sup> This in turn will affect the oxidative capacity of the atmosphere.

Past atmospheric  $\text{NO}_x$  emission levels can be estimated by analyzing  $\text{NO}_3^-$  levels in ice core records. This is because gaseous and particulate  $\text{NO}_3^-$  is traditionally considered the chemical end point of the  $\text{NO}_x$  cycle; however,  $\text{NO}_3^-$  can be converted back into  $\text{NO}_x$  by  $\text{NO}_3^-$  photolysis through the process of renoxification.<sup>24</sup> This phenomenon thwarts our understanding the  $\text{NO}_x$  emission of past atmospheres,<sup>8,12,14</sup> because renoxification alters the  $\text{NO}_3^-$  levels in ice core records of the past atmosphere which is why it is important to explore  $\text{NO}_3^-$  reactivity.

In aqueous solutions and ice conditions,  $\text{NO}_3^-$  photolysis has two channels:



The efficiency of each channel is quantified by its quantum yield, which indicates how many product molecules are formed per photon absorbed by nitrate. Results can range from: 0 (never a reaction) to 1 (always a reaction). However, measuring quantum yields for these two channels is complicated by secondary chemistry where one can observe: photolysis of  $\text{NO}_2^-$  to  $\text{NO}$ , oxidation of  $\text{NO}_2^-$  by hydroxyl radicals to form  $\text{NO}_2$ , or a reaction of  $\text{NO}_2$  with superoxide to form  $\text{NO}_2^-$ .<sup>6,10,22</sup> We will be studying  $\text{NO}_3^-$  photolysis by measuring  $\text{NO}_2^-$  from channel 2 since it is easier to measure than  $\text{NO}_2$ , which is a gas. Furthermore, measuring the  $\text{NO}_2^-$  quantum yield from channel 2 is adequate to studying  $\text{NO}_3^-$  photolysis since both channels are similar based on Benedict's work.

## 1.1 Different regions in ice and its effects:

Chemicals in snow typically reside in three regions: 1. the air-ice interface (otherwise known as the quasi-liquid layer or QLL), 2. liquid-like regions (at the surface of internal air bubbles or at joint boundaries), and 3. the bulk ice matrix (solid solution). When sunlight reacts with chemicals in snow, the reaction rates may vary among the different regions. McFall's et al.<sup>20</sup> shows that the  $\text{NO}_2^-$  quantum yield from  $\text{NO}_3^-$  photolysis ( $2.39 \pm 0.24$ )% is enhanced by a factor of 3.7 at the air-ice interface in comparison to in LLRs.  $\text{NO}_2^-$  quantum yields from  $\text{NO}_3^-$  photolysis in various media are highest at the air-ice interface (QLL)<sup>17,18,20</sup>. Similar results appear in our previous work with guaiacol where there is a 17- to 77-fold increase in the rate constant at the air-ice interface of nature-identical snow compared to in aqueous solution.<sup>17</sup> However, it is unclear what the rate constant of  $\text{NO}_3^-$  photolysis is at the air-ice interface on nature-identical snow since McFall et. al. only worked with ice pellets. Therefore, our research will be determining the quantum yield of photoformed  $\text{NO}_2^-$  from nitrate at the air-ice interface of nature-identical snow.

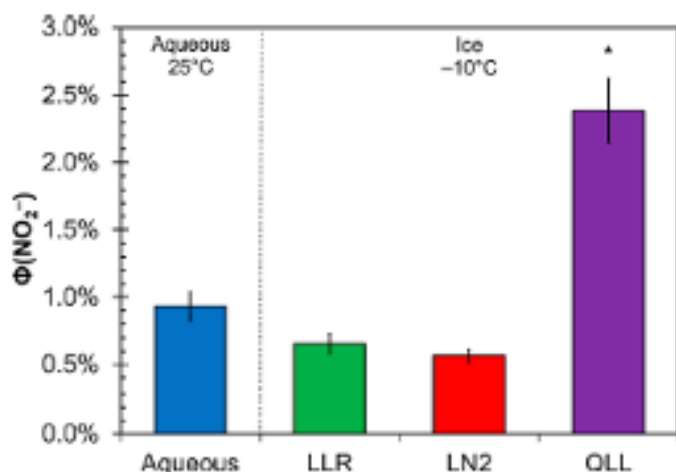


**Figure 1.** McFall’s results show  $\text{NO}_2^-$  quantum yields for nitrate in aqueous and ice forms. Solutes in ice were measured by placing it at the liquid like region (LLR) or the quasi-liquid layer (QLL) and freezing solutes with liquid nitrogen (LN2). All samples were placed under an arc lamp at 313 nm. Figure from McFall, Alexander S., et al. “Nitrate Photochemistry at the Air–Ice Interface and in Other Ice Reservoirs.” *Environmental Science & Technology*, vol. 52, no. 10, 2018, pp. 5710–5717.

## 1.2 Ice pellets vs Snow:

Past experiments have tried to reproduce the physical reaction environment of snow by employing various methods such as: freezing aqueous solutions in molds, turning solutions into ice pellets by spraying into liquid nitrogen, or grinding solute-containing ices into small pieces.<sup>17</sup> Unfortunately, these methods do not replicate impurity-containing natural snow. For example, McFall studied nitrate photolysis in ice pellets but there were problems encountered in the variability of nitric acid ( $\text{HNO}_3$ ) deposited and surface pH.<sup>20</sup> The variability of  $\text{HNO}_3$  created a high acidity of the quasi-liquid layer which made any photoformed  $\text{NO}_2^-$  either become protonated into HONO or oxidized by hydroxyl radicals. Therefore this tampers with understanding how  $\text{NO}_3^-$  photodecays if the target chemical for analysis ( $\text{NO}_2^-$ ) is being lost. To circumvent this issue, subsequently depositing ammonia minimized HONO formation by raising the pH and acting as a scavenger for any hydroxyl radicals.<sup>13,21</sup>

“Surface concentrations of  $\text{HNO}_3$  varied by up to a factor of 4 on a given experiment day” according to McFall et al. due to the ice pellet’s specific surface area (the ratio of sample surface area to ice mass) being  $<1 \text{ cm}^2 \text{ g}^{-1}$ ,<sup>17</sup> thus increasing the chance of chemical aggregation when vapor depositing chemicals onto ice surfaces. In comparison, new natural snow has a specific area of approximately  $1000 \text{ cm}^2 \text{ g}^{-1}$ ,<sup>23</sup> so using ice pellets as a model for snow photochemistry is not ideal. The nature-identical snow that we produce is a more accurate representation of nitrate photochemistry in snow as the specific surface area is much higher at around  $600 \text{ cm}^2 \text{ g}^{-3}$  (snow surface area/ water volume).<sup>23</sup> Furthermore, photodegradation in snow-covered regions occur in snowpacks and not on monolithic surfaces (ice pellets).

Based on our knowledge, this is the first use of nature-identical snow to study photodegradation of nitrate at the air-ice interface. Hullar et. al.<sup>16</sup> have researched the reaction rates of guaiacol in nature-identical snow which has yielded faster reaction rates at the air-ice interface in

comparison to ice pellets. In addition, the natural-identical snow was a more sensitive and useful tool to study air-ice reactions. Hopefully we will get similar results when measuring  $\text{NO}_3^-$  photolysis in the same medium for us to find the quantum yield of  $\text{NO}_2^-$  at the air-ice interface. But doing these experiments requires very low background levels of nitrite in the snow, which might be difficult to achieve given that our snow production room is contaminated with  $\text{NO}_2^-$ . Therefore, our other goal is to reduce background  $\text{NO}_2^-$  levels so that it does not tamper with our measurements.

## 2. Methods

### 2.1 Materials:

We used the following solutions: 15.8M nitric acid, ammonium hydroxide, MQ water, sulfanilamide, N-(1-naphthyl)ethylenediamine dihydrochloride (NEDD), sodium nitroferricyanide (0.5% weight/volume), phenol-ethanol reagent (10% w/v), 2-nitrobenzaldehyde (2-NB, 98% w/v), 5% sodium hypochlorite (Clorox), and alkaline citrate solution: sodium citrate dihydrate (20% w/v) and sodium hydroxide (1% w/v).

### 2.2 Snow making:

Nature-identical snow is made via a custom-built machine,<sup>23</sup> is placed within a cold room at -20°C where we vaporize and nucleate MQ water to form snow. The machine operates for about 96 hours to reduce nitrite contamination present in the snow.

### 2.3 Nitrate deposition:

A nitrogen tank placed in the cold room introduces a flow of nitrogen through a series of containers in our deposition system: First, a pretreatment phase with an HDPE wide-mouth 500 ml bottle filled halfway with snow. This is to put water vapors into the nitrogen stream otherwise a direct flow of nitrogen gas into our snow sample could evaporate the snow. Second, the wide-mouth 500 ml bottle is connected to a glass tube that contains 2ml of stock nitric acid solution to deposit nitrate. Third, another HDPE wide-mouth 500 ml bottle is connected to the glass tube which is filled to the top with snow and is treated with nitric acid from the second container. We deposit nitric acid for 15 minutes at a flow rate of 0.5 litres per minute and then swap out the glass tube with 2 ml of stock ammonium hydroxide for 2 minutes at a flow rate of 0.5 litres per minute. This subsequent introduction of ammonium hydroxide increases the snow's surface pH, minimizes HONO formation, and provide  $\text{NH}_3$  as a scavenger for  $\cdot\text{OH}$ .<sup>19</sup> Lastly, the flow of nitrogen exits through a charcoal canister connected to a SCFH flow meter to ensure there is no blockage in the stream of nitrogen.

### 2.4 Snow collection

The treated snow sample from the third container is placed into a threaded tub of 12.7 centimeters in diameter and 15.24 centimeters in height for “tumbling”. We rotate the tub by inverting it from top to bottom 25 times to ensure that the snow sample is homogeneous. Snow is then put into 16 ten milliliter beakers that are compacted with three successive plugs varying in depth. For example, a beaker is filled to the top with snow and then a plug tamps down the snow. This is repeated two more times with each plug getting shorter in depth. This is done to ensure that each snow sample has the same density while light passes through during the illumination

process. The beakers of snow are covered in either polyurethane (Glad) or nylon film and secured with rubber O-rings.

### 2.5 Illumination:

The 16 beakers are transferred upright into a drilled 4x4 aluminum block to maximize heat distribution and reduce the heat absorbed from the illumination source. The aluminum block is placed in a temperature-controlled cooling chamber at a temperature of  $-15^{\circ}\text{C}$ . 8 dark controls are covered with aluminum foil. Samples were illuminated with a filtered 1000W arc lamp to simulate polar sunlight. Based on previous research,<sup>17</sup> three optical filters are used for the lamp to accurately replicate polar sunlight: an AM 1.5 airmass filter (Sciencetech), a 295 nm longpass filter to remove short wavelengths (250-290 nm), and a 400 nm shortpass filter to remove longer wavelengths from causing sample heating. Samples are pulled out in pairs (an illuminated and dark sample) and are allowed to completely melt at room temperature in dark conditions. Each sample beaker is then partitioned and transferred into HPLC autosampler vials where three separate tests are conducted with various reagents.

### 2.6 Analysis of Nitrite, Nitrate, and Ammonia

To test for  $\text{NO}_2^-$ , a Griess reagent is added to a 750  $\mu\text{L}$  sample to create an azo-dye complex for absorbance measurements.<sup>20</sup> Color development time requires 10 minutes after adding 20  $\mu\text{L}$  of sulfanilamide followed by an additional 10 minutes after adding 20  $\mu\text{L}$  of NEDD. The reacted sample is analyzed by pushing samples through a 100cm pathlength, Liquid Waveguide Capillary Cell by World Precision Instruments and absorbance measurements are taken through a TIDAS spectrophotometer. We run a standard for  $\text{NO}_2^-$  with concentrations of 0nM, 10nM, 25nM, 50nM, 100nM, and 150nM then use Beer's law to determine the concentration of  $\text{NO}_2^-$  from each sample.

$\text{NO}_3^-$  is tested with a solution of vanadium chloride (III) and Griess reagent<sup>7</sup> by a 1:1 sample:testing solution. We added 300  $\mu\text{L}$  of the vanadium chloride (III) and Griess reagent solution with 300  $\mu\text{L}$  of melted snow sample. This sample must be allowed to sit for 16 hours before it can be analyzed.

Testing for  $\text{NH}_3$  consists of taking 500  $\mu\text{L}$  of sample and adding 20  $\mu\text{L}$  of sodium nitroferricyanide, 20  $\mu\text{L}$  of the phenol-ethanol reagent, and 50  $\mu\text{L}$  of oxidizing solution (2.5 mL of 5% sodium hypochlorite and 10 mL of the alkaline citrate solution). Color development requires 5 hours before analysis. Both samples prepared to test for  $\text{NO}_3^-$  and  $\text{NH}_3$  are automatically analyzed through our Shimadzu High Performance Liquid Chromatography.

### 2.7 Actinometry:

2-nitrobenzaldehyde (2NB) is used as a chemical actinometer to account for differing photon fluxes among experimental days and sample preparation methods.<sup>11,18</sup> Illuminating 10  $\mu\text{M}$  2NB at  $0-5^{\circ}\text{C}$  will give us  $j_{2\text{NB}}$  (rate constant for loss of 2NB) as a reference for  $j(\text{NO}_3^- \rightarrow \text{NO}_2^-)$  (rate constant of nitrate loss/ nitrite formation). We measure  $j_{2\text{NB}}$  for each experimental preparation except for when we experiment with snow. Previous research within our research group found the ratio of 2-NB in snow to aqueous measurements:  $0.38 \pm 0.015$  (1 SD) for 10ml beakers.<sup>17</sup> Using this ratio as well as the measured aqueous  $j_{2\text{-NB}}$  on a given experimental day will give us an approximation of snow  $j_{2\text{-NB}}$  for that day.

## 2.8 Calculating rate constants:

We determined the photodegradation rate constant similarly to Hullar et al.<sup>18</sup> where we took the natural logarithm of the ratio of each nitrate concentration at time  $t$  to the initial nitrate concentration. We would then adjust the ratio by multiplying it with the photon-flux correction factor for each sample position. The slope of the regression line through these points gives the pseudo-first-order rate constant for loss during illumination,  $j(\text{NO}_3^- \rightarrow \text{NO}_2^-)$ . Doing a similar calculation to the dark controls will provide us with the rate constant for dark loss,  $k'(\text{NO}_3^- \rightarrow \text{NO}_2^-)$ . Subtracting the dark rate constant from  $j(\text{NO}_3^- \rightarrow \text{NO}_2^-)$  yields the dark-corrected photodegradation rate constant,  $j(\text{NO}_3^- \rightarrow \text{NO}_2^-)_{\text{exp}}$ . Lastly, this constant is divided by  $j_{2-\text{NB}}$  measured that day to give us the photon flux-normalized photodegradation rate constant,  $j^*(\text{NO}_3^- \rightarrow \text{NO}_2^-)$ .

## 3. Results

### 3.1 Nitrite contamination:

An issue that we encountered while vapor depositing nitric acid and ammonia onto our natural-identical snow was the high  $\text{NO}_2^-$  contamination in the cold room. This complicates our  $\text{NO}_2^-$  measurements that come directly from  $\text{NO}_3^-$  photolysis because the LWCC that we used to measure  $\text{NO}_2^-$  concentrations could not show readings greater than 200nM. In addition, we also wanted to see at least a 10 percent increase in the  $\text{NO}_2^-$  concentration from the initial to the final time point. If we already had a high concentration of  $\text{NO}_2^-$ , it would take too long to see an observable increase in  $\text{NO}_2^-$  given the time it takes for  $\text{NO}_3^-$  to photolyze into  $\text{NO}_2^-$  is slow.

Therefore, our solution to reducing the background  $\text{NO}_2^-$  concentration in our cold room was to clean the room by running the snow machine for long periods of time. In addition, charcoal activated filters were attached to the snow machine to prevent  $\text{NO}_2^-$  from getting circulated back into the snow. We ran the snow machine for 96 hours in three different weeks and two months into the process, we can see the baseline is almost close to zero (Figure 2 and Figure 3). Recent measurements of  $\text{NO}_2^-$  levels in the cold room yield values that range from 55-60 nM.

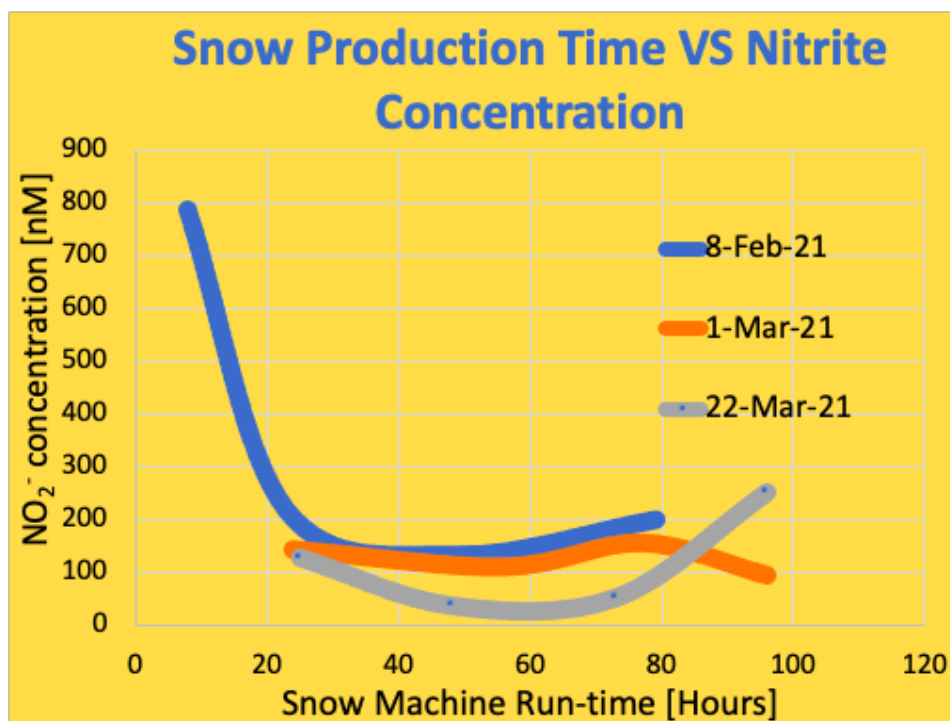


**Figure 2.** Three different weeks recorded for NO<sub>2</sub><sup>-</sup> contamination in the cold room. The lowest NO<sub>2</sub><sup>-</sup> concentration in February was between 100-150 nM and by running the snow machine for 96 hours per week, we were able to reduce the NO<sub>2</sub><sup>-</sup> concentration to nearly 0 nM by late March.

Week of 8-Feb-2021		Week of 1-Mar-2021		Week of 22-Mar-2021	
Snow production duration (hrs)	NO <sub>2</sub> <sup>-</sup> concentration (nM)	Snow production duration (hrs)	NO <sub>2</sub> <sup>-</sup> concentration (nM)	Snow production duration (hrs)	NO <sub>2</sub> <sup>-</sup> concentration (nM)
8	788	24	142	25	129
24	217	56	109	48	38
49	132	77	155	73	53
79	199	96	93	96	235

**Figure 3.** Each table shows the three different weeks from Figure 2 with snow production duration (hrs) and its corresponding NO<sub>2</sub><sup>-</sup> concentration (nM).

### 3.2 Nitrite formation in the dark:

As a control, we had a set of samples in dark conditions to ensure that NO<sub>2</sub><sup>-</sup> production was directly from NO<sub>3</sub><sup>-</sup> photolysis. If there is an observed increase in NO<sub>2</sub><sup>-</sup> from our control, we know that there are other factors that can either produce NO<sub>2</sub><sup>-</sup> or contaminate our samples with additional NO<sub>2</sub><sup>-</sup>. Unfortunately, we experienced an increase in NO<sub>2</sub><sup>-</sup> with our dark controls but



we are unable to determine what is the main source for this phenomenon. However, we have changed our illumination method to reduce  $\text{NO}_2^-$  formation in our controls. This will be discussed further below.

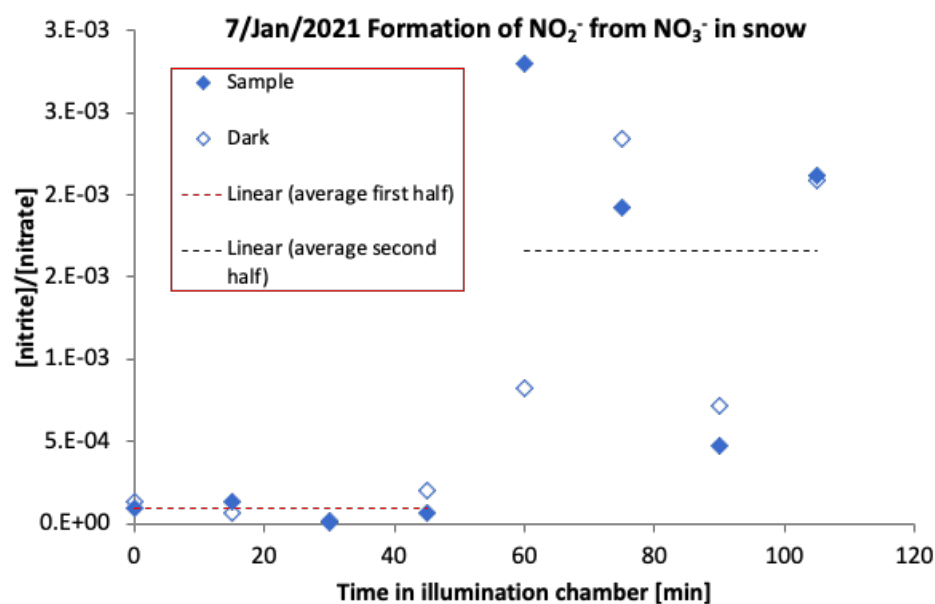


**Figure 4.** Illuminated (solid blue diamond) and dark control (hollow diamond) samples were not exposed to light for 45 minutes. After 45 minutes, all samples were exposed to light however the dark controls also exhibited an increase in  $\text{NO}_2^-$  levels. Each sample was normalized by dividing  $\text{NO}_2^-$  by  $\text{NO}_3^-$  to reduce variability.

### 3.3 Vapor Deposition inconsistencies:

Another issue that we are encountering is an inconsistency in  $\text{HNO}_3$  and  $\text{NH}_3$  deposition onto the snow. We are successful in depositing  $\text{HNO}_3$  with an average concentration of 61  $\mu\text{M}$  and a relative standard deviation of 0.68. Whereas for the average concentration of  $\text{NH}_3$  deposition, is 1873  $\mu\text{M}$  with a relative standard deviation of 0.72. Currently, we are altering the duration of deposition as well as the flow rate to hopefully increase the concentration of  $\text{HNO}_3$  and reduce  $\text{NH}_3$  concentration.

## 4. Future Research

### 4.1 Illumination with the MIS monochromator

Our current method of illuminating snow samples with the filtered 1000W arc lamp is not working which may explain why we are not getting different  $\text{NO}_2^-$  production levels in the illuminated samples than the controls. Upon inspection, the 1000W arc lamp's light intensity is not sufficient for noticeable  $\text{NO}_2^-$  production levels. Therefore, we have transitioned to using the MIS monochromator that McFall et. al.<sup>20</sup> used when measuring quantum  $\text{NO}_2^-$  yields on ice pellets. The MIS monochromator has a higher photon flux and reactions should be 20 times faster given that we can illuminate  $\text{NO}_3^-$  samples with the specific range of 313 nm. Figure 5 shows the photoformation rate of  $\text{NO}_2^-$  from an experiment we conducted with light (14.996 nM/min) and dark control samples (-4.0143 nM/min). This indicates that the MIS works given

that the dark control is not forming any  $\text{NO}_2^-$  while the light samples are. Figure 6 also shows the photoformation of  $\text{NO}_2^-$  in the same experiment but it has been corrected for background  $\text{NO}_3^-$ . The data is not a perfect linear function but with more experiments, we hope to improve our results.

#### 4.2 Sample containers

The sample containers have also been changed to polymethyl methacrylate in place of the 10mL beakers and each sample time points are illuminated individually.

#### 4.2 Preliminary Quantum Yields

We have recorded a  $\text{NO}_2^-$  quantum yield of 1.82%  $\pm$  0.78 using the MIS monochromator with a background  $\text{NO}_2^-$  level of 238 nM. In contrast, McFall et. al.<sup>20</sup> observed a quantum yield of 0.65  $\pm$  0.07% at the LLR at 10°C and 2.39  $\pm$  0.24% at the air-ice interface at 10°C. However, the exact quantum yield of  $\text{NO}_2^-$  in nature identical snow requires more experiments to be conducted.

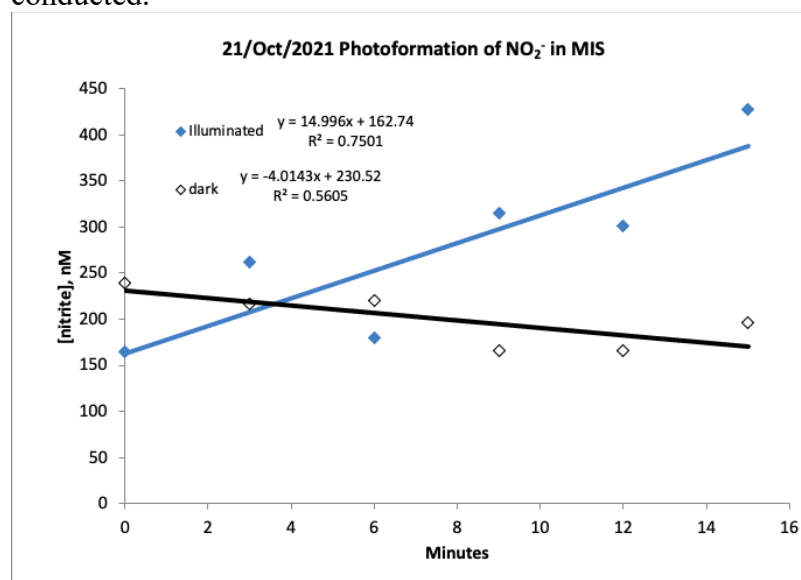


**Figure 5.** Early results of  $\text{NO}_2^-$  production using the MIS monochromator. Not corrected for background  $\text{NO}_3^-$ .

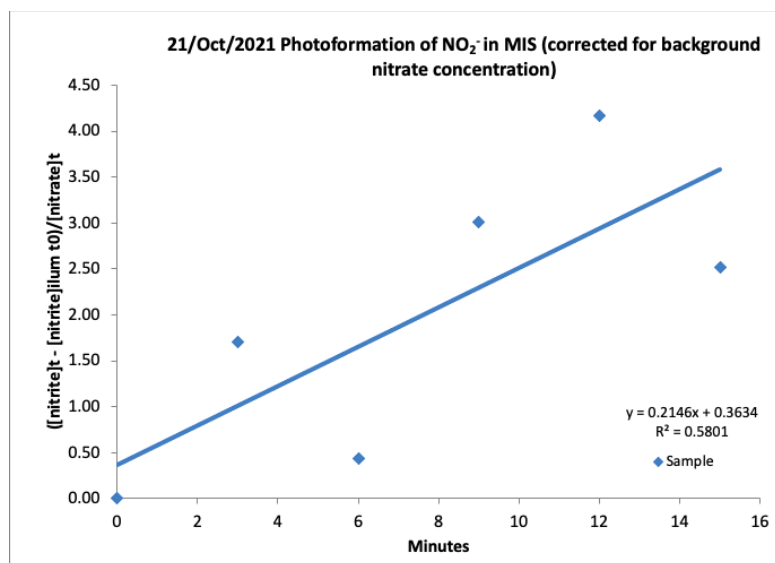


**Figure 6.** Same results as Figure 5 but is corrected for the initial nitrate concentration.

## • References

- Anastasio, Cort, and Liang Chu. "Photochemistry of Nitrous Acid (HONO) and Nitrous Acidium Ion ( $\text{H}_2\text{ONO}^+$ ) in Aqueous Solution and Ice." *Environmental Science & Technology*, vol. 43, no. 4, 2009, pp. 1108–1114.
- Anastasio, Cort, et al. "Photochemistry in Terrestrial Ices." *The Science of Solar System Ices*, 2012, pp. 583–644.
- Benedict, Katherine B., and Cort Anastasio. "Quantum Yields of Nitrite ( $\text{NO}_2^-$ ) from the Photolysis of Nitrate ( $\text{NO}_3^-$ ) in Ice at 313 Nm." *The Journal of Physical Chemistry A*, vol. 121, no. 44, 2017, pp. 8474–8483.
- Boxe, C. S., et al. "Kinetics of NO and  $\text{NO}_2$  Evolution from Illuminated Frozen Nitrate Solutions." *The Journal of Physical Chemistry A*, vol. 110, no. 10, 2006, pp. 3578–3583.
- Boxe, C. S., and A. Saiz-Lopez. "Multiphase Modeling of Nitrate Photochemistry in the Quasi-Liquid Layer (QLL): Implications for  $\text{NO}_x$  release from the Arctic and Coastal Antarctic Snowpack." *Atmospheric Chemistry and Physics*, vol. 8, no. 16, 2008, pp. 4855–4864.
- Chu, Liang, and Cort Anastasio. "Temperature and Wavelength Dependence of Nitrite Photolysis in Frozen and Aqueous Solutions." *Environmental Science & Technology*, vol. 41, no. 10, 2007, pp. 3626–3632.
- Doane, Timothy A., and William R. Horwath. "Spectrophotometric Determination of Nitrate with a Single Reagent." *Analytical Letters*, vol. 36, no. 12, 2003, pp. 2713–2722.
- Domine, F. "Air-Snow Interactions and Atmospheric Chemistry." *Science*, vol. 297, no. 5586, 2002, pp. 1506–1510.
- Finlayson-Pitts, Barbara J., and James N. Pitts. "Applications of Atmospheric Chemistry." *Chemistry of the Upper and Lower Atmosphere*, 2000, pp. 871–942.
- Fischer, M; Warneck, P. "Photodecomposition of Nitrite and Undissociated Nitrous Acid in Aqueous Solution." *The Journal of Physical Chemistry*, vol. 100, no. 48, 1996, pp. 18749–18756.
- Galbavy, Edward S., et al. "2-Nitrobenzaldehyde as a Chemical Actinometer for Solution and Ice Photochemistry." *Journal of Photochemistry and Photobiology A: Chemistry*, vol. 209, no. 2-3, 2010, pp. 186–192.
- Grannas, A. M., et al. "An Overview of Snow Photochemistry: Evidence, Mechanisms and Impacts." *Atmospheric Chemistry and Physics*, vol. 7, no. 16, 2007, pp. 4329–4373.
- Hickel, B., and K. Sehested. "Reaction of Hydroxyl Radicals with Ammonia in Liquid Water at Elevated Temperatures." *International Journal of Radiation Applications and Instrumentation. Part C. Radiation Physics and Chemistry*, vol. 39, no. 4, 1992, pp. 355–357.
- Hoffmann, Michael R. "Possible Chemical Transformations in Snow and Ice Induced by Solar (UV PHOTONS) and Cosmic Irradiation (MUONS)." *Chemical Exchange Between the Atmosphere and Polar Snow*, 1996, pp. 353–377.
- Honrath, R. E., et al. "Evidence of  $\text{NO}_x$  production within or upon Ice Particles in the Greenland Snowpack." *Geophysical Research Letters*, vol. 26, no. 6, 1999, pp. 695–698.
- Hullar, Ted, et al. "Enhanced photodegradation of dimethoxybenzene isomers in/on ice compared to in aqueous solution." (Submitted for publication)
- Hullar, Ted, et al. "Photodecay of Guaiacol is Faster in Ice, and Even More Rapid on Ice, than in Aqueous Solution." *Environmental Science: Processes & Impacts*, vol. 22, no. 8, 16 July 2020, pp. 1666–1677.

18. Hullar, Ted, et al. "Photodegradation Rate Constants for Anthracene and Pyrene Are Similar in/on Ice and in Aqueous Solution." *Environmental Science & Technology*, vol. 52, no. 21, 2018, pp. 12225–12234.
19. Liao, W., and D. Tan. "1-D Air-Snowpack modeling of atmospheric nitrous acid at South Pole during ANTCI 2003." *Atmospheric Chemistry and Physics*, vol. 8, no. 23, 2008, pp. 7087–7099.
20. McFall, Alexander S., et al. "Nitrate Photochemistry at the Air–Ice Interface and in Other Ice Reservoirs." *Environmental Science & Technology*, vol. 52, no. 10, 2018, pp. 5710–5717.
21. Men'kin, V, et al. "Pulse Radiolysis Study of Reaction Rates of OH and O<sup>•</sup> Radicals with Ammonia in Aqueous Solutions." *High Energy Chemistry (English Translation)*, vol. 22, 1989, pp. 333–336.
22. Scharko, Nicole K., et al. "Release of Nitrous Acid and Nitrogen Dioxide from Nitrate Photolysis in Acidic Aqueous Solutions." *Environmental Science & Technology*, vol. 48, no. 20, 2014, pp. 11991–12001.
23. Schleef, Stefan, et al. "An Improved Machine to Produce Nature-Identical Snow in the Laboratory." *Journal of Glaciology*, vol. 60, no. 219, 2014, pp. 94–102.
24. Shi, Qianwen, et al. "Laboratory Investigation of Renoxification from the Photolysis of Inorganic Particulate Nitrate." *Environmental Science & Technology*, vol. 55, no. 2, 2021, pp. 854–861.
25. Thomas, J. L., et al. "Modeling Chemistry in and above Snow at Summit, Greenland – Part 1: Model Description and Results." *Atmospheric Chemistry and Physics*, vol. 11, no. 10, 2011, pp. 4899–4914.